Supporting Information

Coufal et al. 10.1073/pnas.1100273108

SI Methods

Animals. Long interspersed element-1–enhanced green fluorescent protein (L1–EGFP) transgenic animals have been previously described (1). Ataxia telangiectasia mutated (ATM) knockout (KO) mice were kindly provided by Carolee Barlow (independent consultant) (2). The L1–EGFP transgene was incorporated into the ATM KO background by crossing L1–EGFP males to $ATM^{+/-}$ females. L1–EGFP $ATM^{+/-}$ females were then crossed with $ATM^{+/-}$ males. The L1–EGFP transgene consists of a human full-length retrotransposition-competent $L1_{RP}$ element tagged with a *mEGFPI* retrotransposition indicator cassette (3). To analyze L1 retrotransposition in $ATM^{-/-}$ mice, six aged-matched male mice from the same C57BL/6J background were used per group. Quantification of EGFP-positive cells in whole-brain slices was done by individuals blinded to mouse genotypes. EGFP-positive cells were counted in a one-in-six series of sections (~240 μm apart). Images were taken by a *z*-step of 1 μm using a Bio-Rad Radiance 2100 confocal microscope. All experimental procedures and protocols were approved by the Animal Care and Use Committee of The Salk Institute and University of California San Diego.

Primers used for genotyping were as follows. To analyze the L1 transgene, Fw (GCACCATCTTCTTCAAGGAC) and Rv (TCTTTGCTCAGGGCGGACTC) were used. A 1,243-bp band indicates the L1 transgene with intron, and a 343-bp product from tail genomic DNA indicates a germ line or early embryonic insertion event. To determine ATM allele status, the primers Fw (GACTTCTGTCAGATGTTGCTGCC), Rv (CGAATTTGCAGGAGTTGCTGAG), and Neo (GGGTGGGATTAGATAAATGCCTG) were used. The wild-type allele amplifies a 162-bp product, whereas the neomycin insertion transgene is a 441-bp product; cycling conditions were as previously described (2).

Adult animals (4–5 wk old) were killed with an overdose of anesthetics (a mixture of 75 mg/kg ketamine, 10 mg/mL rompun, and 5.6 mg/kg acepromazine) and perfused transcardially with cold 4% paraformaldehyde in phosphate buffer (0.1 M, pH 7.4). The brains and other organs were removed and stored in the fixative overnight. Next, the organs were transferred into 30% sucrose and cut after an additional 48 h. Brains were cut coronally (40 μm) on a sliding microtome from a dry ice-cooled block. Sections were stored at −20 °C in cryoprotectant containing 25% ethylene glycol, 25% glycerin, and 0.05 M phosphate buffer. For immunofluorescence, tissue sections were washed three times in Tris buffered saline (TBS) and blocked for 1 h at room temperature. Primary antibodies were applied in TBS with 3% donkey serum and 0.3% Triton X-100 overnight at 4 °C. Sections were then washed in TBS, blocked for an additional hour, and incubated with the secondary antibodies for 2 h at room temperature before mounting. Antibody dilutions were used as described below (immunofluorescence and immunoblotting). Images were taken by a *z*-step of 1 μm using a Bio-Rad Radiance 2100 confocal microscope.

Plasmid DNA Constructs. ***small hairpin RNA vectors.*** siRNAs were commercially available and purchased from Invitrogen. siRNAs were transfected into human embryonic stem cells (hESCs) using the Amaxa electroporation system, nucleofector solution V, and program A-24. Cells were harvested at 3 d for Western blotting. Once specific siRNAs were confirmed to decrease ATM expression, shRNAS were constructed using 70-bp oligonucleotides matching the siRNAs along with complementary oligos (all purchased from IDT) and annealed by boiling and slow cooling. Annealed products were cloned into the lentiviral pDEST backbone (Invitrogen) and confirmed by sequencing.

Hairpin sequences were as follows, with the control being a scrambled sequence that would form a hairpin: ATM1 (GCAACATTTGCCTATATCAGCAATTTTCGAATTGCTGATATAGGCAAATGTTGCGGTG), ATM2 (GCGCAGTGTAGCTACTTCTTCTATTTTCGAATAGAAGAAGTAGCTACACGCGCGGTG), and ATM3 (GCACTGACCTCTGTGACTTTTCGAAGTCACAGAGGTCAGTGCGGTG).

Long interspersed element-1 vectors. Cloning strategies are available upon request. All long interspersed element-1 (LINE-1) vectors were constructed using a modified version of pCEP4 (Invitrogen) that lacks the CMV promoter and contains a puromycin resistance gene instead of a hygromycin selection gene (3) unless otherwise indicated. DNA superhelicity was confirmed by electrophoresis on 0.7% agarose–ethidium bromide gels, and only highly supercoiled preparations of DNA (>90%) were used in transfection experiments.

L1 plasmid constructs: *cpL1.3mEGFPI* (referred to as L1.3–EGFP) contains an 8.7-kb NotI-BamHI fragment containing a full-length L1.3 element (4, 5) and a *mEGFPI* retrotransposition indicator cassette (3).

cpL1.3D205AmEGFPI (referred to as L1.3–D205A–EGFP) is a derivative of cpL1.3mEGFPI that contains a missense mutation (Asp205Ala) in the endonuclease domain of ORF2 (introducing an FspI restriction site) (5).

cpL1.3H230AmEGFPI (referred to as L1.3–H230A–EGFP) is a derivative of cpL1.3mEGFPI that contains a missense mutation (His230Ala) in the endonuclease domain of ORF2 (introducing an NheI restriction site) (5).

cpL1.3D702AmEGFPI (referred to as L1.3–D702A–EGFP) is a derivative of cpL1.3mEGFPI that contains a missense mutation (Asp702Ala) in the reverse transcriptase domain of ORF2 (introducing a PvuII restriction site) (5).

cpL1.3RR261-62AAmEGFPI (referred to as L1.3–JM111–EGFP) is a derivative of cpL1.3mEGFPI that contains two missense mutations (ArgArg261-62AlaAla) in the RNA-binding domain of the ORF1-encoded protein (3, 6).

cpLRE3mEGFPI (referred to as LRE3–EGFP) has been described previously (7). It contains an 8.7-kb NotI–BamHI fragment containing a full-length LRE3 element (8) and a *mEGFPI* retrotransposition indicator cassette (3).

cpLRE3H230AmEGFPI (referred to as LRE3–H230A–EGFP) is a derivative of cpLRE3mEGFPI that contains a missense mutation (His230Ala) in the endonuclease domain of ORF2 (introducing an NheI restriction site).

cpL1RPRR261-62AAmEGFPI (referred to as L1RP–JM111–EGFP) has been described previously (3, 6). Briefly, it contains a full-length human L1RP element (9) that contains two missense mutations (ArgArg261-62AlaAla) in the RNA-binding domain of the ORF1-encoded protein.

*cpLRE3*mEGFPI* (referred to as LRE3*–EGFP) contains an 8.7-kb NotI–BamHI fragment containing a full-length LRE3 element (8) and a *mEGFPI* retrotransposition indicator cassette (3). The *Bam*H1 site in ORF2 had been silently mutated.

cpLRE3-B1-mEGFPI* (referred to as LRE3*B1–EGFP) is a derivative of cpLRE3*mEGFPI that contains a 500-bp ColE1 sequence (10) between the mEGFPI cassette and the SV40 polyadenylation signal from the modified pCEP4.

cpLRE3-B2-mEGFPI* (referred to as LRE3*B2–EGFP) is a derivative of cpLRE3*–B1–mEGFPI that contains two 500-bp

ColE1 sequences cloned between the mEGFPI cassette and the SV40 polyadenylation signal from the modified pCEP4.

ColE1 was amplified by PCR with the primers Fw: (GCGGTAATACGGTTATCCACAGAA) and Rv: (TCAATCTAAAGTATATATGAGTA), which were flanked by either BamHI sites and a restriction site for SfiI or by two SfiI sites. The first ColE1 copy was introduced using the BamHI site; the second ColE1 was introduced by way of the introduced SfiI site into *cpLRE3*-B1-mEGFPI*.

Luciferase constructs: *pGL3-L1-5′ UTR* has been described previously (1, 7, 11). It contains the 900-bp 5′ UTR promoter region of a human L1.3 element (4) cloned in vector pGL3-basic (Promega).

pGL3-synapsin1 has been described previously (7). It contains the 526-bp synapsin-1 promoter region (a kind gift from G. Thiel, University of Cologne, Germany) cloned in pGL3-basic (Promega).

Luciferase Assays. Luciferase assays were performed as previously described (7). Luciferase activity was measured with the Dual-Luciferase reporter assay system according to instructions provided by the manufacturer (Promega). In all assays, a plasmid expressing the Renilla *luciferase* gene was used as an internal control. The assays were replicated independently at least three times.

Ribonucleoprotein Particle Isolation and Western Blot Analysis. Ribonucleoprotein particles (RNPs) were isolated and analyzed as previously described (12). Briefly, hESCs or neural progenitor cells (NPCs) were harvested and lysed as previously described with 1 mL of 1.5 mM KCl, 2.5 mM $MgCl_2$, 5 mM Tris·HCl (pH 7.4), 1% deoxycolic acid, 1% Triton X-100, and 1× Complete Mini EDTA-free Protease Inhibitor mixture (Roche) (12). Cell debris was removed by centrifugation at 3,000 × *g* at 4 °C for 5 min, and 10% of the supernatant fraction was saved [i.e., the whole-cell lysate (WCL) fraction]. A sucrose cushion then was prepared with 8.5% and 17% wt/vol sucrose in 80 mM NaCl, 5 mM $MgCl_2$, 20 mM Tris·HCl (pH 7.5), and 1 mM DTT, which was supplemented with 1× Complete Mini EDTA-free Protease Inhibitor mixture (Roche). WCLs were centrifuged at 39,000 × *g* for 2 h at 4 °C using a Sorvall SW-41 rotor. After centrifugation, the pelleted material (i.e., the RNP sample) was resuspended in 50 μL of purified water supplemented with 1× Complete Mini EDTA-free protease inhibitor mixture (Roche). Total protein concentration was determined by Bradford assay according to instructions provided by the manufacturer (Bio-Rad). WCL and/or RNP samples (8 μg of each sample) were loaded on 10% SDS/PAGE gels (Bio-Rad). Antibodies and dilutions were as follows: anti-ORF1, rabbit polyclonal antibody, 1:10,000 dilution (a generous gift from Thomas Fanning, National Institutes of Health, Bethesda, MD); anti-S6 ribosomal protein, rabbit polyclonal antibody, 1:1,000 dilution (Cell Signaling); and anti-Sox1, goat polyclonal, 1:500 dilution (R&D). All HRP-conjugated secondary antibodies were used at a 1:20,000 dilution (Abcam).

Western blotting was carried out using standard protocols. Protein concentrations were estimated by performing Lowry Assays (Bio-Rad), and 30 μg of protein was loaded per well. The following antibodies were used at the indicated dilutions: rabbit anti-ATM (1:2,500) (Epitomics); rabbit anti-actin (1:5,000) (Sigma), and rabbit anti-Sox2 (1:5,000) (Chemicon). All secondary antibodies were purchased from Jackson ImmunoResearch.

Cell Culture, Transfection, and Analysis. NPCs were derived from hESCs as previously described (7, 13). NPCs were transfected by nucleofection (Amaxa Biosystems) and either maintained as progenitors in the presence of fibroblast growth factor 2 (FGF2) or differentiated as previously described (7).

The hESC line HUES6 was cultured as previously described (http://www.mcb.harvard.edu/melton/HUES/) (7, 14). Under our experimental conditions, both control and ATM-deficient hESCs exhibited a grossly normal karyotype, as did derived NPCs (Fig. S3). Briefly, cells were grown on Matrigel-coated plates (BD Biosciences) in DMEM media (Invitrogen) supplemented with 20% KO serum replacement, 1 mM L-glutamine, 50 μM β-mercaptoethanol, 0.1 mM nonessential amino acids, and 10 ng/mL FGF2. The cells were passaged by a combination of manual dissection using the StemPro EZPassage passaging tool (Invitrogen) and a brief treatment with trypsin.

Lentiviral virus-like particles were produced as previously described (15). Briefly, recombinant lentiviruses were produced by transient transfection of HEK293T with three packaging vectors in addition to the pDEST shRNA vector. The control virus used is pDEST, which contains a shRNA toward a scrambled target sequence. Infectious media were harvested, filtered, and concentrated by ultracentrifugation. Efficacy of lentivirus was tested by infection of HUES6 hESCs at varying viral concentrations and subsequently by Western blotting.

The hESCs were passaged by a combination of manual dissection and trypsin and subsequently washed in PBS. A suspension of single cells was collected in a microcentrifuge tube and briefly centrifuged, and all but 20 μL PBS was removed. Ten microliters of high-titer lentivirus was added and mixed with the hESCs. The cells were incubated for 20–30 min at 37 °C and subsequently plated in hESC media. Once cells had recovered (at ∼1 wk), they were plated at low density to a 10-cm plate. Post infection, cells were selected with 2 μg/mL blasticidin beginning 4 d after infection and lasting for a minimum of 10 d. Thereafter, single colonies were manually selected. These colonies were grown and later tested by Western blot analysis for expression of ATM. Thirty colonies were selected for each ATM and control shRNA, and 15 that exhibited robust growth and normal hESC colony morphology were tested by Western blot analysis for expression of SOX2 and ATM. More than 90% of ATM shRNA-infected colonies exhibited robust knockdown of ATM. Three to five lines with robust ATM knockdown were selected for each shRNA construct and for control, were tested to confirm normal karyotype, and were differentiated to NPCs. Those with the best differentiation were selected for further analysis, were two control lines. hESCs were reselected with blasticidin after every three passages.

For embryoid body (EB) formation, cells were grown to large colony size and then manually scraped. They were then grown for 7 d in DMEM-F12 Glutamax media (Invitrogen) with N2 supplement (Gibco) and 500 ng/mL Noggin (Fitzgerald) in nonadherent petri dishes. The resulting EBs were plated onto laminin/polyornithine (Sigma)-coated plates and were grown for 7–10 d. Rosettes were manually dissected and dissociated in 0.1% trypsin and plated in DMEM-F12 media supplemented with N2 and B-27, 1 μg/mL laminin, and 20 ng/mL FGF2. The resulting NPCs could be maintained for multiple passages before the induction of differentiation. Differentiation conditions involved the withdrawal of mitogens and treatment of the cells with 20 ng/mL of brain-derived neurotrophic factors, 20 ng/mL of glia-derived neurotrophic factors (Peprotech), 1 mM di-butyryl-cyclicAMP (Sigma), and 200 nm of ascorbic acid (Sigma) for 4–12 wk.

HUES6-derived NPCs and human fetal neural progenitor cells (hCNS-SCns) were transfected by nucleofection using the Amaxa rat neural stem cell (NSC) nucleofector solution and program A-31. The transfection efficiency was determined by using cells transfected with an EGFP plasmid and analyzed 2 d post transfection by FACS analysis. The transfection efficiency ranged from 50 to 80% for hESC-derived NPCs and from 50 to 70% for hCNS-SCns. Cells were cultured as progenitors in the presence of mitogens. For differentiation studies, cells were dissociated and plated for differentiation 8–10 d after the initial

transfection. Cells were monitored for EGFP expression by fluorescence microscopy. For FACS analysis, cells were dissociated and analyzed on a Becton-Dickinson LSR I in the presence of 1 μg/mL propidium iodide for live/dead cell gating. All assays were performed in triplicate. JM111–EGFP transfected cells were used as a negative control for gating purposes. Silencing of EGFP expression was determined by addition of either the HDAC inhibitor 500 nM trichostatin-A or the de novo DNA methyltransferase inhibitor 5′ azacytidine at 500 ng/mL for 24 h on day 8 post transfection.

The HCT116 cell line, a colon carcinoma cell line (ATCC), was grown as previously described (16). In brief, cells were cultured in DMEM supplemented with 10% FBS and 1.5 mM L-glutamine. They were passaged with 0.1% trypsin treatment. HCT116 lines deficient in nonhomologous end-joining genes (DNA-$PK_{cs}^{-/-}$, DNA ligase $IV^{-/-}$, and $XLF^{-/-}$) were a kind gift from Matthew Weitzman (The Salk Institute, La Jolla, CA). ATM-deficient HCT116 lines were made by plating HCT116 or HCT116 $p53^{-/-}$ cells at low density (20%) in a six-well plate and then infecting overnight with 5 μL of high-titer lentivirus (ATM shRNA or control shRNA) in 1 mL of media. Cells were subsequently replated at low density to a 10-cm dish, and single colonies were selected for expression analysis and further experiments. Infection efficiency was >85% with a GFP-containing lentivirus. The dominant-negative p53 (DNp53) construct was a kind gift from Geoffrey Wahl (The Salk Institute, La Jolla, CA). The ATR and Mre11 shRNA plasmids in the shUpf1 plasmid were a kind gift from Matthew Weitzman. The BRCA1 shRNA in the pGEM-T plasmid was a kind gift from Inder Verma (The Salk Institute, La Jolla, CA). For BRCA1, ATR, and MRE11 shRNA experiments and for experiments using the DNp53, HCT116 cells were plated in six-well plates and then transfected the following day using Lipofectamine (Invitrogen) per the manufacturer's protocol. For RT-PCR experiments, cells were harvested 3 d post transfection. For L1 retrotransposition assays, cells were transfected again 2 d after the initial transfection with the L1 plasmids and then assayed 5 d later for L1–EGFP expression.

The hCNS-SCns lines were cultured as previously described and were a kind gift from Stem Cells (Palo Alto, CA) (7, 17). hCNS-SCns cells were derived from fetal brain by FACS using the cell-surface markers $(CD133)^+$, $(5E12)^+$, $(CD34)^-$, (CD45), and $CD24^{-/lo}$. This combination of markers enriches for progenitor neurosphere-initiating cells capable of differentiating into cells of both the neuronal and glial lineages (17). The hCNS-SCns cells were cultured in X-Vivo 15 media (Lonza BioScience) supplemented with 20 ng/mL FGF2, 20 ng/mL epidermal growth factor, 10 ng/mL leukemia inhibitor factor, N2 supplement, 0.2 mg/mL heparin, and 60 μg/mL *N*-acetylcysteine.

Karyotype analysis was performed by Cell Line Genetics and also performed in-house as previously described (18). Briefly, cells were incubated overnight in demecolcine solution (#D1925; Sigma) at 10 ng/mL and then harvested in EDTA/Versine with the slow addition of 75 mM KCL. Cells were incubated and then fixed with the addition of a 3:1 methanol:glacial acetic acid solution. Cells were then spread on a slide, rapidly flame dried, and stained with Vectashield with DAPI (Vector Laboratories). Chromosome spreads were identified using fluorescent microscopy, photographed, and quantified.

Cell cycle staining was performed as previously described (19, 20). Briefly, cells were trypsinized, washed, and resuspended in PBS buffer and then fixed by addition of a 3:1 ratio of ice-cold 100% ethanol in PBS overnight at −20 °C. Subsequently, cells were washed and resuspended in a solution containing 50 μg/mL propidium iodide and 500 ng/mL RNase A for 1 h at 37 °C before analysis by FACS on a Becton-Dickinson FACScan.

Electrophysiology. ATM and control shRNA-infected HUES6-hESCs were differentiated to neural rosettes; the best rosettes were manually selected and dissociated, grown for a single passage as NPCs, electroporated with the LRE3–EGFP plasmid, allowed to proliferate for 8 additional days, and subsequently differentiated, as previously described (7). Whole-cell perforated patch recordings were performed on EGFP-expressing cells after 12–13 wk of differentiation. The recording micropipettes (tip resistance 3–6 MΩ) were tip-filled with internal solution composed of 115 mM K-gluconate, 4 mM NaCl, 1.5 mM $MgCl_2$, 20 mM Hepes, and 0.5 mM EGTA (pH 7.4) and then backfilled with the same internal solution containing 200 μg/mL amphotericin. Recordings were made using an Axopatch 200B amplifier (Axon Instruments). Signals were sampled and filtered at 10 and 2 kHz, respectively. The whole-cell capacitance was fully compensated, whereas the series resistance was uncompensated but monitored during the experiment by the amplitude of the capacitive current in response to a 5-mV pulse. The bath was constantly perfused with fresh Hepes-buffered saline composed of 115 mM NaCl, 2 mM KCl, 10 mM Hepes, 3 mM $CaCl_2$, 10 mM glucose, and 1.5 mM $MgCl_2$ (pH 7.4). For current-clamp recordings, cells were clamped between ~ −60 to −80 mV. For voltage-clamp recordings, cells were clamped at −70 mV. All recordings were performed at room temperature. Amphotericin B was purchased from Calbiochem. All other chemicals were from Sigma.

PCR and RT-PCR. Adult human tissues from patients with ataxia telangiectasia (AT) and age- and sex-matched controls ($n = 7$ for each group) were obtained from the National Institutes of Child Health & Human Development (NICDH) Brain and Tissue Bank for Developmental Disorders (University of Maryland, Baltimore). Experiments were performed on an ABI Prism 7000 sequence detection system (Applied Biosystems). Whole-genome size was estimated using the following equation: cell genomic DNA content = 3×10^9(# bp) × 2(diploid) × 660 (molecular weight 1 bp) × 1.67×10^{12} (weight 1 Da), resulting in the approximation that one cell contains 6.6 pg genomic DNA (21). For each tissue, 10-μM sections were generated and stained for neuronal nuclei (NeuN) (1:100). For each tissue, 100 cells were laser captured on an Arcturus PixCell IIE Laser Capture Microdissection Instrument, and the genomic DNA was extracted using the PicoPure DNA Extraction Kit, according to the manufacturer's instructions, with triplicate identical laser capture samples. The genomic DNA from 100 cells was resuspended in 50 μL, and 5 μL was used per genomic DNA qPCR reaction, which is equivalent to 10 cells per reaction and comparable to the 12 cells/reaction used in previous studies (7, 18).

Oligonucleotide PCR primers were purchased from Allele Biotech and TaqMan-MGB probes were obtained from Applied Biosystems and were designed using Primer Express software (Applied Biosystems). L1 primers were verified using the L1 database (http://l1base.molgen.mpg.de/) and matched a minimum of 140 of 145 full-length L1s with two intact ORFs in the database.

Quantitative PCR experiments were performed using an ABI Prism 7000 sequence detection system and Taqman Gene Expression Mastermix (Applied Biosystems). Data analysis was performed with SDS 2.3 software (Applied Biosystems). The multiplexing reaction was optimized by limiting reaction components until both reactions amplified as well as each individual reaction. Standard curves of genomic DNA ranging from 2 ng to 16 pg were performed to verify that the ~70-pg dilution used was within the linear range of the reaction. Primer efficiency and multiplexing effectiveness were verified by linear regression to the standard curve and indicated a slope near −3.32, representing acceptable amplification of both PCR products and matched primer efficiencies. ORF2 probes were conjugated to the fluorophore label VIC, and all other probes were conjugated with 6FAM. For the control assay depicted in Fig. 5*E* (HERVH/SATA), the HERVH probe was generated with the VIC fluorophore to multiplex with the SATA-6FAM probe set. Copy numbers were

determined using the University of Calfornia at Santa Cruz genome browser in silico PCR function, and the primers and probes used were the following: primers (7)—HERVH (99 copies), probe (5′-CCCTTCGCTGACTCTC-3′), Fw (5′-AATGGCCCCACCCCTATCT-3′), and Rv (5′-GCGGGCTGAGTCCGAAA-3′); 5S RNA (35 copies), probe (5′-AGGGTCGGGCCTGG-3′), Fw (5′-CTCGTCTGATCTCGGAAGCTAAG-3′), and Rv (5′-GCGGTCTCCCATCCAAGTAC-3′); SATA [millions of copies (22)], probe (5′-TCTTCGTTTCAAAACTAG-3′), Fw (5′-GGTCAATGGCAGAAAAGGAAAT-3′), and Rv (5′-CGCAGTTTGTGGGAATGATTC-3′); L1 ORF2 (4,560 copies), probe (5′-CTGTAAACTAGTTCAACCATT-3′), Fw (5′-TGCGGAGAAATAGGAACACTTTT-3′), and Rv (5′-TGAGGAATCGCCACACTGACT-3′).

Copy-number estimates are based on previously described methodologies (7). The increase in L1 ORF2 genomic DNA content is 2–3% in AT patients compared with controls. First, the L1 ORF2 primers described above match ∼4,500 copies of L1 in the human genome according to the University of California at Santa Cruz genome browser. Therefore, an increase of 2% would be equivalent to ∼90 copies of L1 per hippocampal neuronal genome. Second, we have previously published spiking experiments (7) in which we spiked a calculated copy number of L1 plasmid into somatic tissue to measure the quantity required to increase the somatic tissue to the L1 copy-number level of hippocampal tissue. We calculated an increase of ∼80 L1 copies per hippocampal genome with a concomitant increase of 3–7% in the quantity of genomic L1 DNA in the qPCR assay. The spiked L1 copies were in the form of a plasmid, which likely affects the copy-number estimates, providing an estimate of relative change and imprecise quantification of the absolute number of L1s per cell. On the basis of this estimate, the increase of 2% that we find in AT patients compared with control would be equivalent to ∼50 copies per hippocampal neuron.

Genomic DNA from transfected ATM-deficient and control NPCs was isolated using the DNeasy Blood and Tissue kit according to instructions provided by the manufacturer (Qiagen). Genomic DNA was collected 10 d post transfection from NPCs. To assay for removal of the intron from the retrotransposition indicator cassette, 200 ng of genomic DNA was used in a 25-μL PCR with the primers EGFP968s and EGFP1013as. PCR cycling conditions were described previously (3, 6). The marker ladder used in all gel pictures is a 1-kb plus ladder (Invitrogen, catalog #10787–081).

Inverse PCR (IPCR) was performed as previously described (7, 23). Briefly, HUES6-derived ATM-deficient and control NPCs were transfected with the native, full-length LRE3 and then allowed to grow for 14 d. The resulting cells were dissociated with trypsin and sorted on a Becton-Dickinson FACscan. A total of 40,000 EGFP-positive cells were sorted for each shRNA. These cells proliferated in culture and, like the EGFP-negative control cultures, expressed the expected neural stem markers (Fig. S7*C*) and could be differentiated to neuronal and glial lineages at similar rates to control cultures (Fig. S7*D*). The cells were harvested, and genomic DNA was isolated using standard phenol–chloroform techniques. Briefly, 5–10 μg of genomic DNA was digested overnight with either SspI or XbaI. The digested DNA then was ligated under dilute conditions in a final volume of 1 mL with 3,200 U of T4 DNA ligase (New England Biolabs) overnight at 4 °C. The circular ligated DNA was concentrated to 50 μL using a Microcon 100 column (Millipore) and then was subjected to IPCR using previously described conditions (7). EGFP primers utilized: 5′-CTTGAAGAAGATGGTGCG-3′ and 5′-ACAACCACTACCTGAGCACC-3′. PCR reactions were carried out with the Expand Long kit using buffer system 1 following the manufacturer's directions (Roche). We used a 5-μL aliquot from this reaction in a second-round nested PCR using the primers 5′-TTGAAGAAGTCGTGCTGC-3′ and 5′-AAAGACCCCAACG AGAAGCG-3′. PCR products were gel-isolated, cloned into the TOPO TA 2.1 plasmid (Invitrogen), and sequenced. Identification of the L1 preintegration sites and other DNA sequence analyses were performed using the University of California at Santa Cruz genome browser (http://genome.ucsc.edu; March 2006 assembly) (24).

For RT-PCR, RNA was isolated from various cell and tissue types with RNABee (Tel-Test) following the manufacturer's directions. RNA quality was verified by gel electrophoresis, and cDNA was synthesized using the cells-to-cDNA II kit (Ambion/Applied Biosystems) per manufacturer's instructions. PCR was carried out using Taq Polymerase (Promega). Cycling parameters were as follows: 94 °C for 1 min and then 25 or 30 cycles with the following parameters: 94 °C for 1 min, 50–60 °C for 1 min, and 72 °C for 1 min. RT-PCR analysis was performed using the following primer pairs:

L1—Fw (GCATTACCATTCAGGACATAGGC) and Rv (GTTCTAGATCCCTGAGGAATCGC); ATM—Fw (ACAACCCCTGCAAACTTGG) and Rv (TCTGGCTCCCCTATACTTCTG); ATR—Fw (AAGCCGTTCTCCAGGAATAC) and Rv (ATCTATCGCCCCCAATTCCC); p53—Fw (TCCCCAGCCAAAGAAGAAAC) and Rv (AGTGCAGGCCAACTTGTTC); MRE11—Fw (GAAGAATGTGCAGCTCTCAC) and Rv (CACTAAAGGCAGAAGCAGAC); BRCA1—Fw (AGTCACTTATGATGGAAGGGTAGC) and Rv (ATC TGGGTGTGAGAGTGAAACAAG); DNA Ligase IV—Fw (TCTGGTTCACAGAGGTAACG) and Rv (TCTGATTTTTTCTGCACGTCC); DNAPKcs—Fw (CGAAGAGCAGCTAGACAACTAC) and Rv (AGGCATAGTTTGCCTTGAGC); XLF—Fw (TCAACAGGTGTGGCATGAAC) and Rv (TGCCCATCAGAGGACGAATC); GAPDH—Fw (CATGTTCGTCATGGGTGTGAACC) and Rv (GGAAATGAGCTTGACAAAGTGGTC); and EGFP—Fw (GCACCATCTTCTTCAAGGAC) and Rv (TCTTTGCTCAGGGCGGACTC).

Immunocytochemistry and Imaging. Cells were fixed in 4% paraformaldehyde, and immunocytochemistry was performed as previously described (7). Antibodies and dilutions were as follows: βIII tubulin, mouse monoclonal, 1:400 or rabbit polyclonal, 1:500 (Babco and Covance); Map (2a+2b), mouse monoclonal, 1:500 (Sigma); glial fibrillary acidic protein (GFAP) rabbit polycolonal, 1:300 (DAKO); GFAP, guinea pig polyclonal, 1:1,000 (Advanced Immunochemical); Nestin, mouse monoclonal, 1:800 (Millipore); tyrosine hydroxylase, rabbit polyclonal, 1:500 (Pel-Freez); Sox2, rabbit polyclonal, 1:500 (Sigma); choline acetyltranserase, rabbit polyclonal, 1:100 (Millipore); EGFP, mouse monoclonal (Molecular Probes and Invitrogen); NeuN, mouse monoclonal, 1:100 (Millipore); GABA rabbit polyclonal, 1:200 (Millipore); synapsin, rabbit polyclonal, 1:50 (Cell Signaling Technology). Secondary antibodies were purchased from Jackson ImmunoResearch or Invitrogen and all were used at 1:250. Cells were imaged using a CARVII spinning disk confocal imaging system (BD).

1. Muotri AR, et al. (2005) Somatic mosaicism in neuronal precursor cells mediated by L1 retrotransposition. *Nature* 435:903–910.
2. Barlow C, et al. (1996) Atm-deficient mice: A paradigm of ataxia telangiectasia. *Cell* 86 (1):159–171.
3. Ostertag EM, Prak ET, DeBerardinis RJ, Moran JV, Kazazian HH Jr. (2000) Determination of L1 retrotransposition kinetics in cultured cells. *Nucleic Acids Res* 28:1418–1423.
4. Sassaman DM, et al. (1997) Many human L1 elements are capable of retrotransposition. *Nat Genet* 16(1):37–43.
5. Wei W, et al. (2001) Human L1 retrotransposition: Cis preference versus trans complementation. *Mol Cell Biol* 21:1429–1439.
6. Moran JV, et al. (1996) High frequency retrotransposition in cultured mammalian cells. *Cell* 87:917–927.

7. Coufal NG, et al. (2009) L1 retrotransposition in human neural progenitor cells. *Nature* 460:1127–1131.
8. Brouha B, et al. (2002) Evidence consistent with human L1 retrotransposition in maternal meiosis I. *Am J Hum Genet* 71:327–336.
9. Kimberland ML, et al. (1999) Full-length human L1 insertions retain the capacity for high frequency retrotransposition in cultured cells. *Hum Mol Genet* 8:1557–1560.
10. Gilbert N, Lutz-Prigge S, Moran JV (2002) Genomic deletions created upon LINE-1 retrotransposition. *Cell* 110:315–325.
11. Athanikar JN, Badge RM, Moran JV (2004) A YY1-binding site is required for accurate human LINE-1 transcription initiation. *Nucleic Acids Res* 32:3846–3855.
12. Kulpa DA, Moran JV (2005) Ribonucleoprotein particle formation is necessary but not sufficient for LINE-1 retrotransposition. *Hum Mol Genet* 14:3237–3248.
13. Zhang SC, Wernig M, Duncan ID, Brüstle O, Thomson JA (2001) In vitro differentiation of transplantable neural precursors from human embryonic stem cells. *Nat Biotechnol* 19:1129–1133.
14. Thomson JA, et al. (1998) Embryonic stem cell lines derived from human blastocysts. *Science* 282:1145–1147.
15. Singer O, et al. (2005) Targeting BACE1 with siRNAs ameliorates Alzheimer disease neuropathology in a transgenic model. *Nat Neurosci* 8:1343–1349.
16. Bunz F, et al. (1998) Requirement for p53 and p21 to sustain G2 arrest after DNA damage. *Science* 282:1497–1501.
17. Uchida N, et al. (2000) Direct isolation of human central nervous system stem cells. *Proc Natl Acad Sci USA* 97:14720–14725.
18. Muotri AR, et al. (2010) L1 retrotransposition in neurons is modulated by MeCP2. *Nature* 468:443–446.
19. Crissman HA, Steinkamp JA (1973) Rapid, simultaneous measurement of DNA, protein, and cell volume in single cells from large mammalian cell populations. *J Cell Biol* 59:766–771.
20. Krishan A (1975) Rapid flow cytofluorometric analysis of mammalian cell cycle by propidium iodide staining. *J Cell Biol* 66:188–193.
21. Forslund O, et al. (2003) Nucleotide sequence and phylogenetic classification of candidate human papilloma virus type 92. *Virology* 312:255–260.
22. Lee C, Wevrick R, Fisher RB, Ferguson-Smith MA, Lin CC (1997) Human centromeric DNAs. *Hum Genet* 100:291–304.
23. Garcia-Perez JL, et al. (2007) LINE-1 retrotransposition in human embryonic stem cells. *Hum Mol Genet* 16:1569–1577.
24. Kent WJ, et al. (2002) The human genome browser at UCSC. *Genome Res* 12: 996–1006.

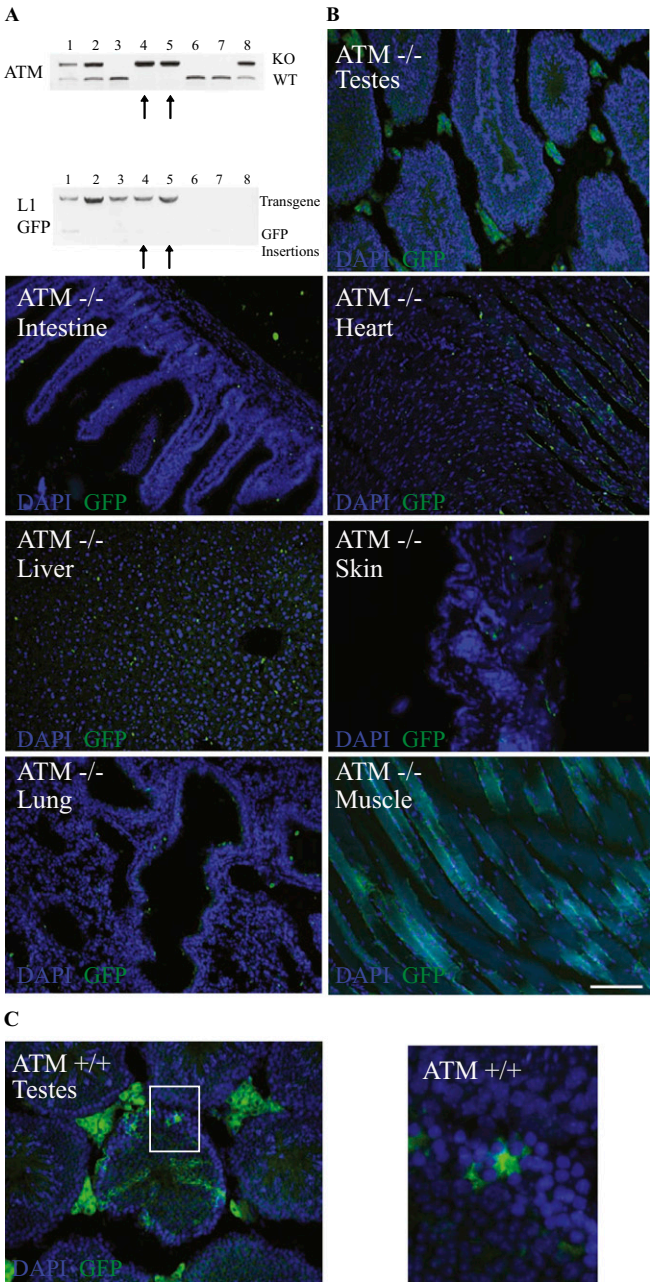

Fig. S1. Detection of L1 retrotransposition in other tissues of L1–EGFP transgenic mice in an ATM KO genetic background. (*A*) Adult transgenic animals carrying the L1–EGFP transgene and homozygous for deletion of ATM were selected for tissue analysis. All tissues were analyzed after staining with an anti-GFP antibody. (Scale bar, 250 μm.) Green in remaining tissues is secondary to autofluorescence visualized in all channels. (*B*) EGFP-positive cells were not identified in somatic tissues, including testes, intestine, heart, liver, skin, muscle, or lung of ATM deficient mice. (*C*) Rare EGFP-positive cells were identified in the testes of L1–EGFP wild-type animals. (*Right*) Magnification of boxed area in *Left* panel).

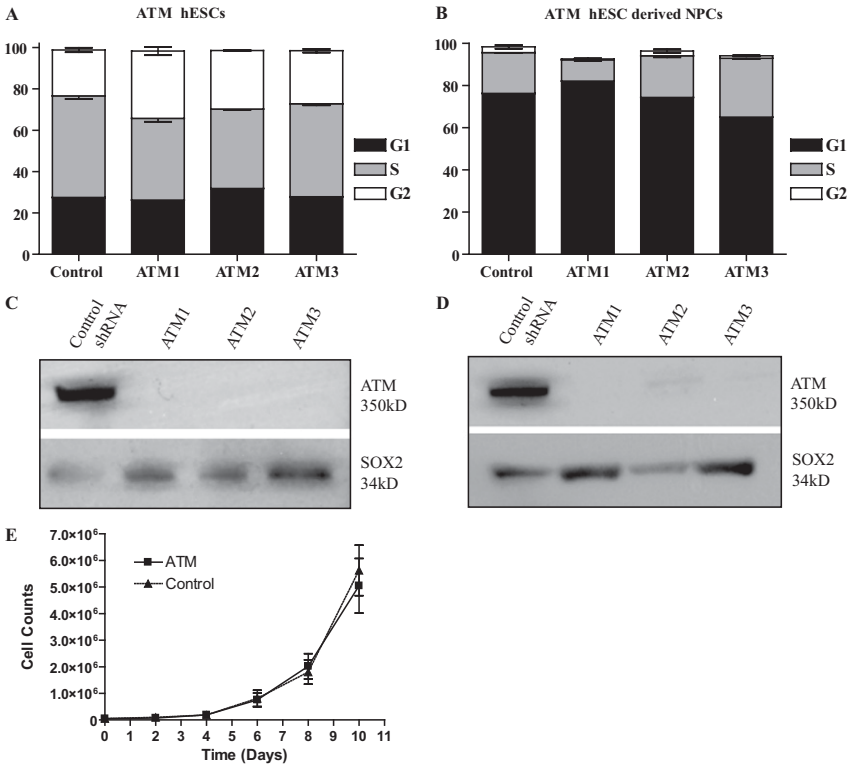

Fig. S2. Characteristics of ATM shRNA-infected cells. (*A*) Cell cycle analysis of ATM-deficient and control HUES6-hESCs indicated no statistically significant difference in cell cycle profiles. (*B*) Similarly, cell cycle analysis of ATM-deficient and control NPCs showed no statistically significant difference in cell cycle profiles. (*C*) Western blotting confirmed the knockdown of ATM in HUES6-hESCs infected with ATM1-3 shRNA lentiviruses, as compared to control shRNA infected cells. (*D*) Western blotting of ATM shRNA-infected human fetal brainstem cells exhibited knockdown of ATM. In *C* and *D*, SOX2 serves as a loading control. (*E*) Growth curves of ATM-deficient and control HUES6-hESC–derived NPCs. We did not observe a statistically significant difference in growth rate.

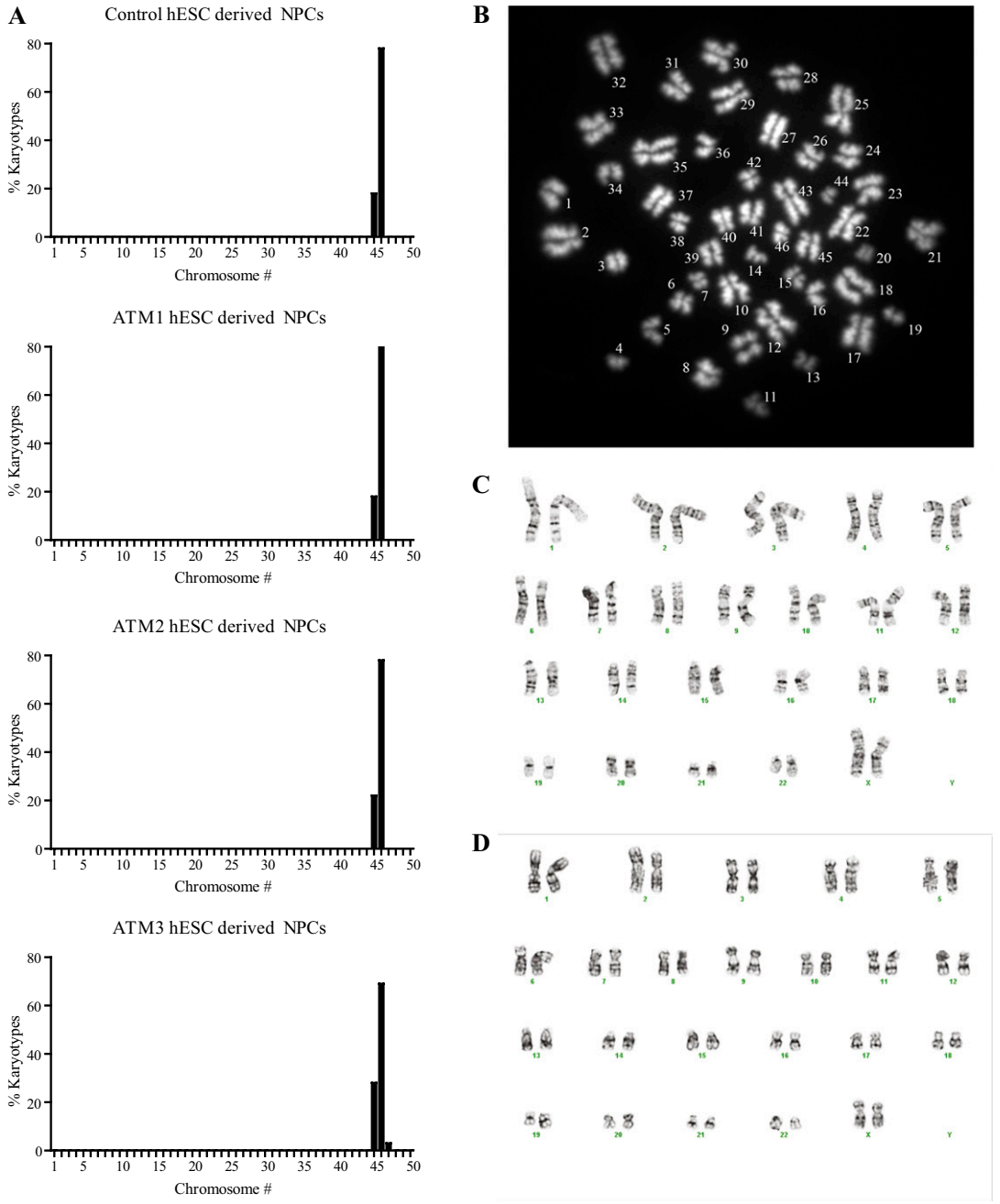

Fig. S3. Karyotype analysis of ATM shRNA- and control lentivirus-infected HUES6-hESCs. (*A*) Karyotype analysis shows no difference in chromosome number between ATM and control shRNA lentivirus-infected HUES6-hESCs (*n* = 100 cells analyzed/sample). (*B*) Representative normal karyotype (ATM2 shRNA). (*C* and *D*) Full karyotype and banding analysis also exhibited normal karyotypes of both control (*C*) and ATM-deficient (*D*) HUES6-hESCs (ATM3 shRNA).

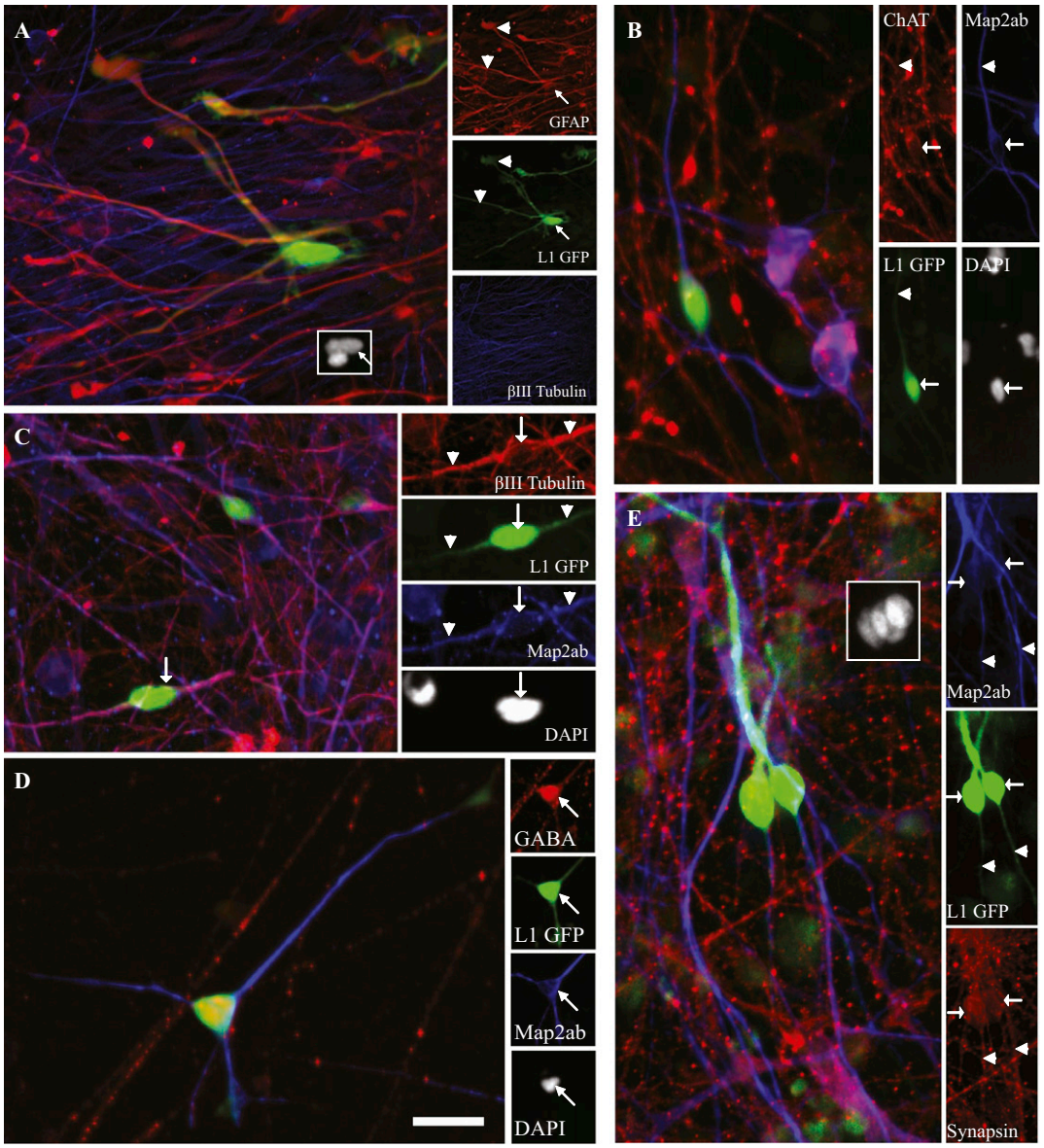

Fig. S4. Further differentiation potential of LRE3–EGFP-positive, ATM-deficient, HUES6-derived NPCs. (*A*) LRE3–EGFP-positive, ATM-deficient, HUES6-derived NPCs can differentiate to a glial cell fate, expressing glial fibrillary acidic protein (GFAP) but not βIII tubulin. (*B–E*) LRE3–EGFP-positive, ATM-deficient, HUES6-derived NPCs can differentiate into neurons expressing general neuronal markers, including Map2a+b, βIII tubulin, and synapsin (*C* and *E*), in addition to subtype-specific neuronal markers such as choline acetyltransferase (ChAT), a marker of cholinergic neurons (*B*), and γ-aminobutyric acid (GABA), a marker of inhibitory GABAergic neurons (*D*). (Scale bar, 25 μm.) Boxed area in *A* and *E* shows DAPI-stained nuclei. Arrows mark colabeled nuclei; arrowheads mark colabeled processes in all panels.

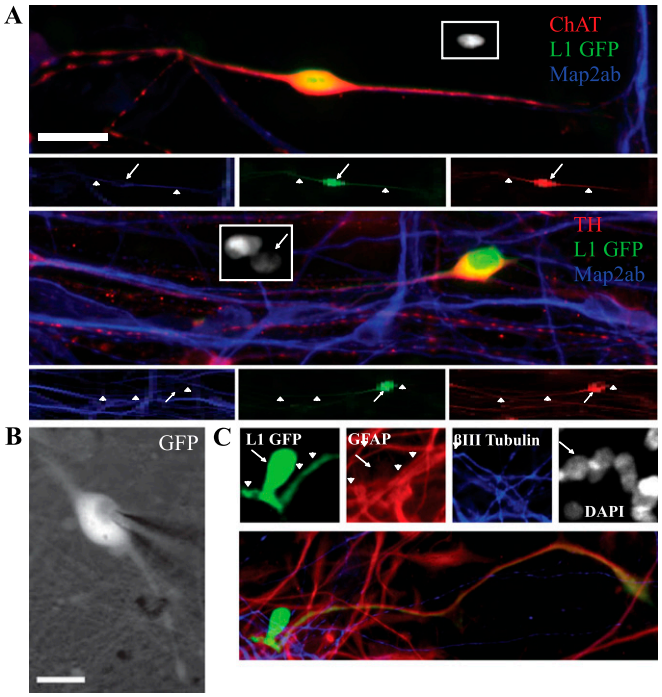

Fig. S5. Differentiation potential of LRE3–EGFP-positive, ATM-deficient, HUES6-derived NPCs. (*A*) LRE3–EGFP-positive, ATM-deficient NPCs can differentiate into neurons that express the neuronal subtype markers choline acetyltranserase (ChAT), indicative of cholinergic neuronal fate, and tyrosine hydroxylase (TH), indicative of a dopaminergic neuronal fate (*Insets*, DAPI nuclear stain). (Scale bar, 2.5 μm.) (*B*) Fluorescence micrograph of a LRE3–EGFP-positive, ATM-deficient (ATM1 shRNA), HUES6-derived neuron from which the data shown in Fig. 2 *F* and *G* were obtained. (Scale bar, 10 μm.) (*C*) LRE3–EGFP-positive, ATM-deficient NPCs can also differentiate to a glial fate, staining for glial fibrillary acidic protein (βIII tubulin-negative). In all immunofluoresence images, arrows indicate colabeled nucleus; arrowheads indicate processes.

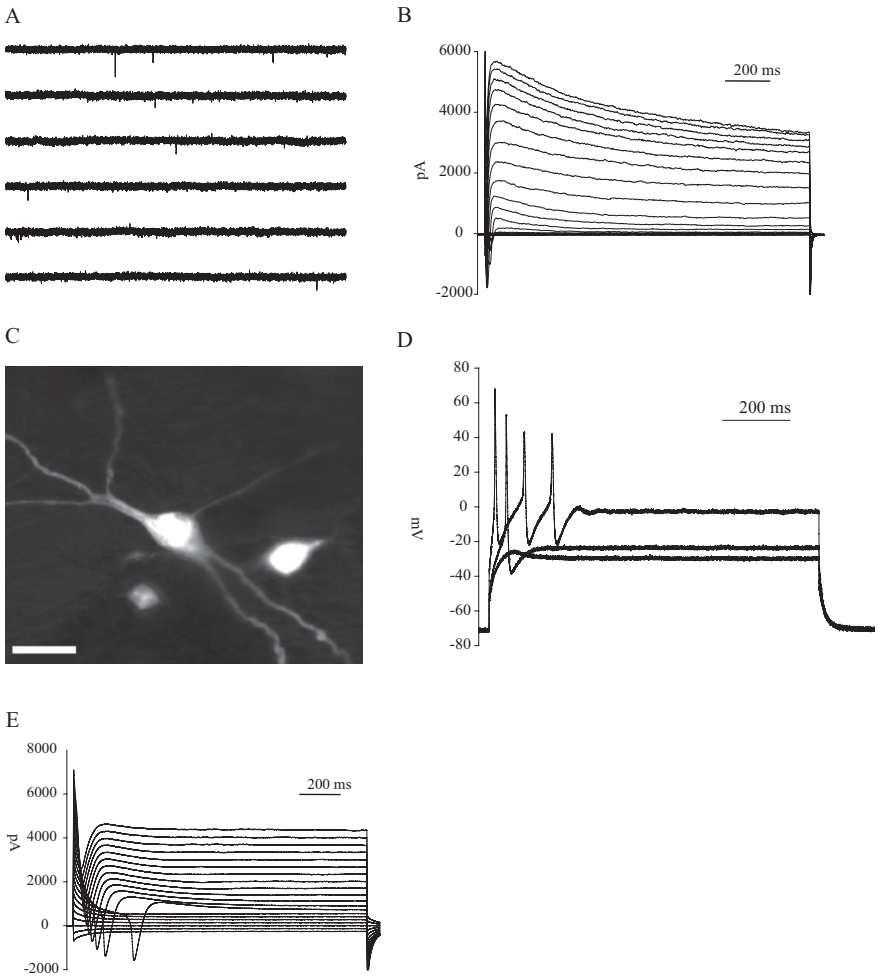

Fig. S6. Electrophysiological activity of LRE3–EGFP neurons in ATM-deficient and control HUES6-derived neurons. (*A*) Spontaneous action potentials in an LRE3–EGFP-positive neuron derived from ATM-deficient HUES6-hESC (ATM3 shRNA). (*B*) Transient Na^+ and sustained K^+ currents in response to 20-mV step depolarizations from a holding potential of −70 mV to potentials ranging from −90 to +100 mV from the same neuron as in *A*. (*C*) Fluorescence micrograph of an LRE3–EGFP-positive neuron expressing the control shRNA lentivirus from which the data in *D* and *E* were obtained. (Scale bar, 10 μm.) (*D*) Suprathreshold responses to somatic current injections from a current clamped potential of −70 mV. (*E*) Transient Na^+ and sustained K^+ currents in response to 20-mV step depolarizations.

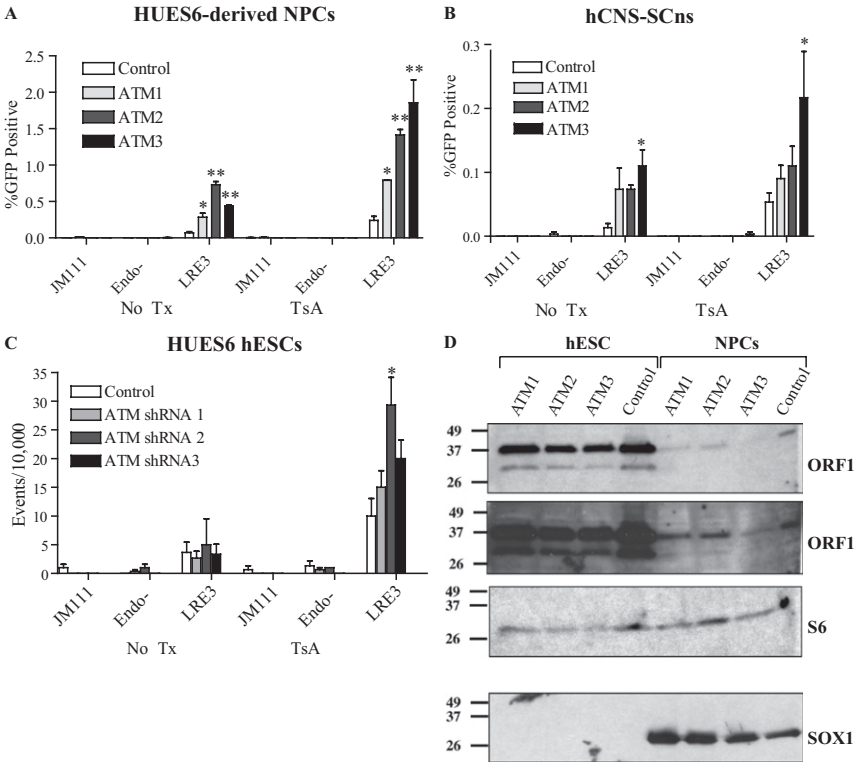

Fig. S7. L1 retrotransposition in other ATM-deficient cell types. (*A*) ATM-deficient NPCs derived from HUES6, (*B*) ATM-deficient hCNS-SCns, and (*C*) ATM-deficient HUES6-hESCs exhibit increased LRE3–EGFP retrotransposition compared with controls, without any evidence of increased endonuclease-independent retrotransposition. Error bars in all panels indicate SEM. $*P < 0.05$ and $**P < 0.01$ are a result of a one-way ANOVA with Bonferroni correction comparing shRNA control cells to ATM1-3 shRNA-expressing cells. (*D*) RNP particles isolated from control and ATM-deficient, HUES6-derived hESCs and NPCs were subjected to Western blotting using anti-ORF1p and antiribosomal S6 antibodies; they showed no significant increase in the amount of L1 RNPs in ATM-deficient cells compared with control. Western blotting from whole-cell lysates for the neural stem cell marker SOX1 shows expression in NPCs but not in hESCs, as predicted. TsA, trichostatin A.

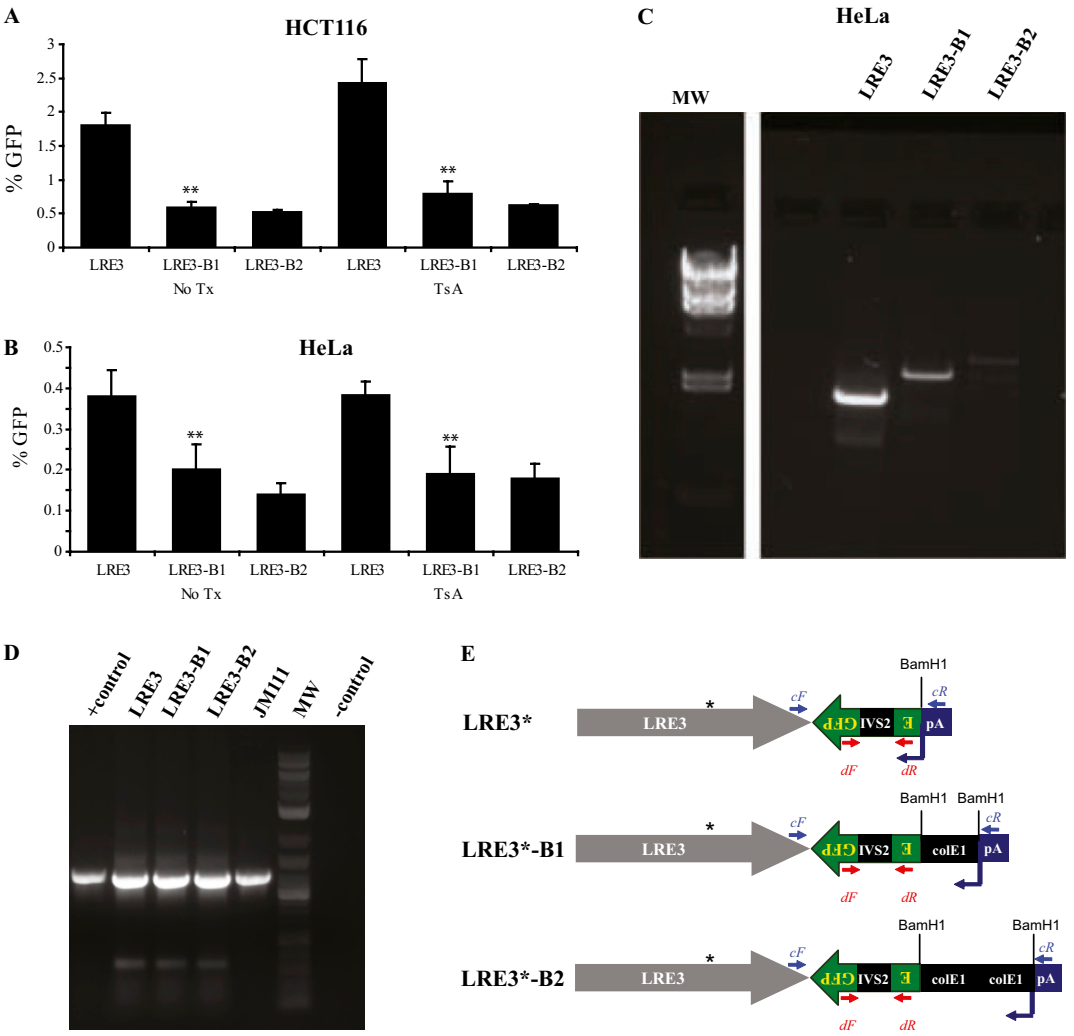

Fig. S8. Verification of the LRE3*–EGFP spacer constructs. HCT116 (*A*) and HeLa (*B*) cells showed a dramatic decrease in L1–EGFP expression after 6 d when transfected with constructs containing one (LRE3*–EGFP–B1) or two (LRE3*–EGFP–B2) 500-bp ColE1 spacers. In all panels, $^{**}P < 0.01$. (*C*) PCR reactions using primers on either side of the indicator cassette (cF and cR in *E*) with genomic DNA derived from transfected HeLa cells indicates that the resultant products are of the expected size (500-bp increase for each copy of ColE1); top bright band is the vector; lower faint band is the retrotransposed product. (*D*) PCR reactions using primers that flank the intron in the EGFP cassette (dF and dR in *E*) with genomic DNA from transfected HeLa cells demonstrated an equally sized EGFP product from all constructs (top bright band is the vector; lower faint band is the retrotransposed product). MW, molecular weight marker. (*E*) Schematic indicating the placement of primers used for the PCR reactions in *C* and *D*. Primers include the forward (cF) and reverse (cR) used in *C* and the forward (dF) and reverse (dR) used in *D*. The asterisk (*) indicates that the parent LRE3 construct has a silent mutation that destroys the BamH1 restriction site in ORF2 (*SI Methods*). Sequences of the PCR primers are available upon request.

Table S1. Insertions characterized by inverse PCR

shRNA	Analysis	5′ sequence*	Poly(A)	EN site	Locus	L1 insertion target site
Control	Full[†]	5248	75	5′-TTGT/AA-3′	12q23	24 kb upstream from SLCA8, solute carrier family 5 (iodide transporter)
Control	Partial	6228	>120	5′-TTTT/TT-3′	9p21	5 kb upstream from IFNA14, IFN, α-14, and into a LINE element
Control	Partial	6229	76	5′-TAAT/AA-3′	8p22	20 kb upstream from NAT1 (*N*-acetyltransferase 1), into a LINE element
ATM1	Partial	6187	44	5′-TTTT/AA-3′	1q32	Into a LINE element
ATM1	Partial	6290	88	5′-ATAT/AA-3′	12p13	Into a SINE element
ATM1	Partial	6254	110	5′-TTTT/AA-3′	1q41	Into an intron of cDNA FLJ34932 (AK092251) and 20 kb upstream from PROX1
ATM1	Partial	5234	>130	5′-TTTT/GT-3′	9p21	5 kb upstream from IFNA14, IFN, α-14, and into a LINE element
ATM1	Partial	6263	78	5′-TTTT/CA-3′	6q14	Into an intron of COL12A1, collagen, type XII, α-1 long isoform
ATM1	Partial	6195	102	5′-TTTT/AA-3′	12q21	>100 kb from any gene
ATM1	Partial	5536	54	5′-TTTT/GT-3′	10q21	Into a LINE element
ATM1	Full[‡]	5286	98	5′-TTTT/GT-3′	4q33	Into a LINE element
ATM1	Partial	6236	31	5′-TTTT/AT-3′	4p16	Into an intron of hypothetical protein LOC152992 isoform 2 (C4orf23) and 20 kb upstream from acyl-CoA oxidase 3, pristanoyl isoform a (peroxidase enzyme)
ATM1	Partial	6226	22	5′-TTTT/CC-3′	3p13	Into an intron of PPP4R2 (protein phosphatase 4)
ATM3	Partial	6258	53	5′-TTTT/GT-3′	2p24	Into a LINE element in a region of ESTs
ATM3	Full[§]	5221	37	5′-TTTT/AA-3′	6q22	80 kb upstream from heparan sulfate (glucosamine)
ATM3	Partial	6018	94	5′-TTTT/AA-3′	1q24	Into an intron of EST *Homo sapiens* cDNA FLJ39010 fis

Three insertions from control shRNA-infected HUES6-derived NPCs, as well as 13 from ATM-deficient, HUES6-derived NPCs (10 from ATM1 and 3 from ATM3) were characterized. Of these insertions, three were characterized at both the 5′ and 3′ ends (one from control, two from ATM-deficient NPCs). The remaining insertions were characterized only on their 3′ end. Notably, all insertions occurred in an actual or inferred A/T-rich endonuclease consensus recognition site.
*For partial insertions, the 5′ sequencing site is the farthest into the L1 that was sequenced. For full insertions, this is the truncation site.
[†]A 1-bp deletion.
[‡]No target site duplication, no deletion.
[§]A 127-bp deletion.